ELSEVIER

Biophysical Chemistry 108 (2004) 89–100

Biophysical Chemistry

www.elsevier.com/locate/bpc

Sedimentation equilibrium in a solution containing an arbitrary number of solute species at arbitrary concentrations: theory and application to concentrated solutions of ribonuclease☆

Silvia Zorrilla[a], Mercedes Jiménez[b], Pilar Lillo[a], Germán Rivas[b], Allen P. Minton[c,*]

[a]*Instituto de Química Física 'Rocasolano', CSIC, Madrid, Spain*
[b]*Centro de Investigaciones Biológicas, CSIC, Madrid, Spain*
[c]*Laboratory of Biochemistry and Genetics, Building 8, Room 226, National Institutes of Health, Bethesda, MD 20892-0830, USA*

Abstract

Simple expressions are derived describing the equilibrium concentration gradient of each species in a solution containing an arbitrary number of solute species at arbitrary concentration, as a function of the concentration of all species. Quantitative relationships between the species gradients and experimentally observable signal gradients are presented. The expressions are model-free and take into account both attractive and repulsive interactions between all species. In order to analyze data obtained from strongly nonideal solutions, a statistical thermodynamic model for repulsive solute–solute interactions is required. The relations obtained are utilized to analyze the dependence of the equilibrium gradient of ribonuclease A in phosphate-buffered saline, pH 7.4, upon total protein concentration. Experimental results are interpreted in the context of a model for weak self-association leading to the formation of significant amounts of oligomers at total protein concentrations exceeding 25 g/l.

Keywords: Thermodynamic nonideality; Reversible association; Ribonuclease

1. Introduction

The technique of sedimentation equilibrium has been extensively applied to detect and quantitate the strength of strong macromolecular self- and hetero-associations that are present in dilute solution [1,2]. Biological fluid media, on the other hand, are generally characterized by a high total concentration of macromolecules (up to several hundred grams per liter), cumulatively occupying a substantial fraction (0.1–0.4) of the total volume of the medium [3,4]. In such media, referred to as 'crowded', the volume excluded by one macromolecule to another is expected to have a substantial and biologically significant effect on the rates and equilibria of biological reactions, including protein assembly processes, involving dilute as well as concentrated macromolecular species [4–7]. It has been suggested that weak macromolecular associations not detectable in dilute solutions might be structurally and functionally important in

☆ This paper is dedicated to David Yphantis in honor of his many contributions to the art and science of analytical ultracentrifugation

*Corresponding author. Tel.: +1-301-496-3604; fax: +1-301-402-0240.

E-mail address: minton@helix.nih.gov (A.P. Minton).

0301-4622/04/$ - see front matter © 2003 Elsevier B.V. All rights reserved.
doi:10.1016/j.bpc.2003.10.012

highly crowded biological environments [4,8]. These considerations motivate attempts to extend the analytical power of sedimentation equilibrium to detect and quantitate macromolecular associations in concentrated or crowded solutions, which are thermodynamically highly nonideal.

Prior extensions of the theory of sedimentation equilibrium that take thermodynamic nonideality into account in an explicit and thermodynamically valid fashion fall into two categories. The first category is based upon expansion of the thermodynamic activity coefficient of each solute species as a power series in the concentrations of all solute species, and the development of inverse expansions of the concentration of each solute species as a function of the activities of all species [9–11]. Treatments in this category become mathematically and computationally intractable with increasing solute concentration and number of solute species due to the difficulty (or impossibility) of deriving and evaluating higher order terms in the expansions. The second category is based upon the use of approximate equations of state of hard particle fluids to evaluate thermodynamic activity coefficients [12–14]. These models are expected to provide a useful and reasonably accurate estimate of the composition-dependent activity coefficients of macromolecules in solutions containing one or more macrosolute species under conditions such that long range electrostatic interactions between macrosolutes are largely damped out [4,15,16]. For simple systems containing only a single concentrated solute species in a buffer of moderate ionic strength, an extended theory of this type was found to be mathematically and calculationally tractable over the entire range of experimentally accessible macrosolute concentrations (up to 200 g/l), and has been used to characterize quantitatively the state of association of dilute fibrinogen, tubulin and FtsZ in concentrated solutions of unrelated macrosolutes [14,17].

In the present work, we extend the treatments of Chatelier and Minton [12,13] and Rivas et al. [14] to the general case of an arbitrary number of interacting solute species at arbitrary concentration. The relations obtained are used to analyze the results of new sedimentation equilibrium experiments carried out on solutions of ribonuclease A (RNase) at concentrations of up to 200 g/l, and to reanalyze previously published results of sedimentation equilibrium experiments carried out on solutions of bovine serum albumin (BSA), aldolase and ovalbumin at concentrations up to 200 g/l [18].

2. Thermodynamic relations governing sedimentation equilibrium

The concentration gradient at sedimentation equilibrium of a single species *i* in a solution containing multiple solute species may be described exactly by the following relation [14]:

$$M^*_{i,\mathrm{app}} = M^*_i - \sum_j w_j \left(\frac{\partial \ln \gamma_i}{\partial w_j} \right) M^*_{j,\mathrm{app}} \qquad (1)$$

where w_i, γ_i, M_i* and $M_{i,\mathrm{app}}$*, respectively, denote the weight/volume concentration, thermodynamic activity coefficient, buoyant molar mass and apparent buoyant molar mass of solute species *i*. The buoyant molar mass M_i* is an experimentally measurable quantity, defined thermodynamically as the product of the actual molar mass times the specific density increment of solute species *i*, measured at constant chemical potential of all solvent species [19]:

$$M^*_i = M_i \left(\frac{\mathrm{d}\rho}{\mathrm{d}w_i} \right)_\mu \qquad (2)$$

where ρ is the solution density expressed in the same units as w/v concentration. The *apparent* buoyant molar mass of solute species *i* is a measure of the concentration gradient of that species at sedimentation equilibrium:

$$M^*_{i,\mathrm{app}} = \frac{2RT}{\omega^2} \frac{\partial \ln w_i}{\partial r^2}. \qquad (3)$$

In a solution containing *n* solute species, the condition of sedimentation equilibrium is fully specified by a set of *n* equations, each of which is obtained by rearranging Eq. (1):

$$\left[1+w_1\left(\frac{\partial \ln \gamma_1}{\partial w_1}\right)\right]M^*_{1,\mathrm{app}}+w_2\left(\frac{\partial \ln \gamma_1}{\partial w_2}\right)M^*_{2,\mathrm{app}}$$

$$+\cdots+w_n\left(\frac{\partial \ln \gamma_1}{\partial w_n}\right)M^*_{n,\mathrm{app}}=M^*_1$$

$$w_1\left(\frac{\partial \ln \gamma_2}{\partial w_1}\right)M^*_{1,\mathrm{app}}+\left[1+w_2\left(\frac{\partial \ln \gamma_2}{\partial w_2}\right)\right]M^*_{2,\mathrm{app}}$$

$$+\cdots+w_n\left(\frac{\partial \ln \gamma_2}{\partial w_n}\right)M^*_{n,\mathrm{app}}=M^*_2$$

……

……

……

$$w_1\left(\frac{\partial \ln \gamma_n}{\partial w_1}\right)M^*_{1,\mathrm{app}}+w_2\left(\frac{\partial \ln \gamma_n}{\partial w_2}\right)M^*_{2,\mathrm{app}}+$$

$$\cdots+\left[1+w_n\left(\frac{\partial \ln \gamma_1}{\partial w_1}\right)\right]M^*_{n,\mathrm{app}}=M^*_n \qquad (4)$$

Given the values of w_i, $\partial \ln \gamma_i/\partial w_j$ and M_i*, Eq. (4) form a set of n linear equations in n unknowns, the $M_{i,\mathrm{app}}$*, which may be rewritten in matrix notation:

$$\underline{\mathbf{A}}\overline{M^*_{\mathrm{app}}}=\overline{M^*}. \qquad (5)$$

In Eq. (5), $\underline{\mathbf{A}}$ denotes a square matrix of dimension $n\times n$, with elements given by

$$\mathbf{A}_{ij}=\delta_{ij}+w_j\left(\frac{\partial \ln \gamma_i}{\partial w_j}\right) \qquad (6)$$

where i is the row index, j the column index and δ_{ij} is the Kronecker delta, equal to 1 when $i=j$ and 0 otherwise. $\overline{M^*_{\mathrm{app}}}$ and $\overline{M^*}$ denote column vectors with $M^*_{\mathrm{app}}(i)=Mi,^*_{\mathrm{app}}$ and $M^*(i)=M_i$*, respectively. Since the w/v concentration w_i is proportional to ρ_i, the number density of molecules of species i,

$$\rho_i(\mathrm{cm}^{-3})=\frac{N_\mathrm{A}}{1000M_i}w_i(\mathrm{g/l}) \qquad (7)$$

Eq. (6) may be rewritten

$$\mathbf{A}_{ij}=\delta_{ij}+\rho_j\left(\frac{\partial \ln \gamma_i}{\partial \rho_j}\right). \qquad (8)$$

The solution to Eq. (5) is then given simply by

$$\overline{M^*_{\mathrm{app}}}=\underline{\mathbf{A}}^{-1}\overline{M^*} \qquad (9)$$

where $\underline{\mathbf{A}}^{-1}$ denotes the matrix inverse of $\underline{\mathbf{A}}$.

Sedimentation equilibrium is experimentally characterized by measuring the equilibrium gradient of at least one *signal* S, which is a composition-dependent property of the solution, such as absorbance at a particular wavelength or refractive index. There may be many such signals (e.g. the absorbance at each of several wavelengths). Assuming that the contribution of each solute species to each signal is proportional to the concentration of that species (an assumption that can and should be checked by the experimenter), the kth signal is then given by

$$S_k(r)=\sum_j \alpha_{k,j}w_j(r) \qquad (10)$$

where $\alpha_{k,j}$ denotes a constant of proportionality (such as an extinction coefficient) between the w/v concentration of species j and the contribution of species j to the kth signal. We may then define a *signal-average buoyant molar mass* for each signal [20] as a simple transformation of the experimentally measured gradient of that signal:

$$M^*_k\equiv\frac{2RT}{\omega^2}\frac{\mathrm{d}\ln S_k(r)}{\mathrm{d}r^2}. \qquad (11)$$

Combination of Eqs. (3) and (11) yields

$$M_k^* = \frac{\sum_j \alpha_{k,j} w_j M_{j,\mathrm{app}}^*}{\sum_j \alpha_{k,j} w_j}. \quad (12)$$

Given the concentration of each solute species (w_j), the buoyant mass of each species (M_i*), the contribution of each species to the measured signal ($\alpha_{k,i}$) and a quantitative measure of interactions between all species ($\partial \ln \gamma_i / \partial w_j$), Eqs. (9) and (12) permit simple calculation of the gradient of signal at sedimentation equilibrium. The values of $\alpha_{k,j}$ and M_i* may be independently measured or estimated as described in Ref. [20]. Calculation of the values of the interaction terms will be described below.

We next consider some commonly encountered special cases resulting in simplification of the general relations given above.

2.1. Special case 1: multiple solute species, thermodynamically ideal

When all macrosolutes are sufficiently dilute, they behave independently, and $\partial \ln \gamma_i / \partial w_j$ approaches 0 for all i and j. Under these conditions matrix **A** reduces to the identity matrix, and $\overline{M_{\mathrm{app}}^*} = \overline{M^*}$. It then follows from Eq. (13) that in a solution containing a single solute component, the signal average buoyant molar mass M_k* reduces to the weight-average buoyant mass

$$M_w^* \equiv \frac{\sum_j w_j M_j^*}{\sum_j w_j} \quad (13)$$

for any signal k, in agreement with the standard textbook result (see, for example, Ref. [21]).

2.2. Special case 2: one solute component, thermodynamically nonideal

In a solution containing only a single solute component (A), all solute species (A_1, A_2,…) present in addition to monomeric A will be formed by self-association. If the amplitude of the kth signal per unit weight/volume concentration of the solute component is independent of its state of association (an assumption that can and should be tested experimentally), then all solute species have the same value of $\alpha_{k,j}$, and Eq. (12) simplifies to

$$M_k^* = \frac{\sum_j w_j M_{j,\mathrm{app}}^*}{\sum_j w_j} = M_{w,\mathrm{app}}^* \quad (14)$$

where $M_{w,\mathrm{app}}$* denotes the weight-average apparent buoyant molar mass, independent of the particular signal used to quantify the equilibrium gradient.

2.3. Special case 3: one solute species, thermodynamically nonideal

In this special case, Eqs. (9) and (12) reduce to the textbook result [21]

$$M_{k,\mathrm{app}}^* = M_{\mathrm{app}}^* = \frac{M^*}{1 + w\left(\frac{\mathrm{d} \ln \gamma}{\mathrm{d}w}\right)}. \quad (15)$$

2.4. Special case 4: two solute species, thermodynamically nonideal

Eq. (4) reduce to expressions originally presented by Chatelier and Minton [13]

$$\left[1 + w_1\left(\frac{\partial \ln \gamma_1}{\partial w_1}\right)\right] M_{1,\mathrm{app}}^* + w_2\left(\frac{\partial \ln \gamma_1}{\partial w_2}\right) M_{2,\mathrm{app}} = M_1^* \quad (16)$$

$$w_1\left(\frac{\partial \ln \gamma_2}{\partial w_1}\right) M_{1,\mathrm{app}}^* + \left[1 + w_2\left(\frac{\partial \ln \gamma_2}{\partial w_2}\right)\right] M_{2,\mathrm{app}}^* = M_2^*. \quad (17)$$

If, in addition, species 1 is dilute, Eq. (16) further

simplifies to

$$M_1^* = M_{1,\mathrm{app}}^* + w_2\left(\frac{\partial \ln \gamma_1}{\partial w_2}\right)M_{2,\mathrm{app}} \quad (18)$$

which is the relation previously utilized by Rivas et al. [14] to analyze data obtained from the measurement of tracer sedimentation equilibrium in highly nonideal solutions.

2.5. Special case 5: multiple solute species, small deviations from thermodynamic ideality

The thermodynamic activity coefficient of each solute species may be expressed as a power series of the concentrations of all solute species

$$\ln \gamma_i = \sum_j B_{ij} w_j + \sum_j \sum_k B_{ijk} w_j w_k + \ldots \quad (19)$$

where successive terms on the right-hand side of Eq. (19) represent contributions from two-body, three-body and higher order interactions to the chemical potential of species *i*. The interaction (or virial) coefficients B_{ij}, B_{ijk},… are functions of the effective potential of interaction between two, three and higher numbers of solute molecules in solution [22]. If it is assumed that deviations from ideality are sufficiently small such that contribution from higher order terms are negligible, then Eq. (6) reduces to

$$\mathbf{A}_{ij} \approx \delta_{ij} + B_{ij} w_j. \quad (20)$$

Since two-body interaction coefficients are symmetric ($B_{ij} = B_{ji}$), there are $n(n+1)/2$ independent coefficients of two-body interaction between n solute species. In the absence of a statistical-thermodynamic model for solute–solute interaction, the B_{ij} may be treated as floating parameters in the context of an overall model for the analysis of data. However, if the overall model contains more than two non-dilute solute species (three two-body interaction coefficients) such a procedure becomes numerically hazardous.

3. General model for self-association and nonideal repulsive interaction in a solution containing a single solute component

Relations presented to this point have been developed from thermodynamic arguments and are therefore model-free. The total intermolecular interaction between solute species in solution may in an entirely general fashion be partitioned into attractive interactions, leading to the reversible formation of complexes treated as distinct species and repulsive interactions, contributing to increases in the chemical potential of each species [23]. Both types of interactions may occur together due to the superposition of different mechanisms of interaction (e.g. electrostatic attraction and steric repulsion). Analysis of sedimentation equilibrium data thus involves two types of model: (1) a model specifying possible states of association and the energetics governing equilibria between them, and (2) a model for repulsive interactions between solute species. A variety of models of both types have been described elsewhere [14,17,24]. Below we present a general model, incorporating both association and repulsive interaction, for calculation of solution composition and signal average buoyant molar mass in a solution containing one solute component, and an algorithm for simultaneously calculating the composition of solute species and signal-average buoyant molar mass of the solute as a function of its total concentration. An instance of this model was used to analyze the data describing sedimentation equilibrium in ribonuclease solutions presented subsequently.

Consider a solution containing macrosolute P, which may exist as monomer in equilibrium with dimer, trimer, etc.[1] We define the thermodynamic association constants for $i > 1$:

$$K_i^o(T,\ P) \equiv \frac{a_i}{{a_1}^i} = \frac{\gamma_i w_i}{(\gamma_1 w_1)^i} \quad (21)$$

[1] In the interest of notational simplicity we have neglected the possible presence of alternate conformers having identical stoichiometry (i.e. species 2a, 2b, etc.). Extension to include such conformers is straightforward, but of secondary interest, as they would ordinarily not be discriminated by sedimentation equilibrium.

where a_i denotes the thermodynamic activity, γ_i the activity coefficient and w_i the weight/volume concentration of i-mer. The ratio of w/v concentrations is given by the apparent equilibrium constant

$$K_i \equiv \frac{w_i}{w_1^i} = K_i^{\circ}\frac{\gamma_1^i}{\gamma_i} \tag{22}$$

and the conservation of mass expressed by

$$w_{\text{tot}} = \sum_i w_i = \sum_i K_i w_1^i. \tag{23}$$

We also specify a functional dependence of the activity coefficients of each species upon the w/v concentration of all species:

$$\ln \gamma_i = f_i(\{w\}). \tag{24}$$

Partial derivatives of the f_i are used to evaluate $(\partial \ln \gamma_i/\partial w_j)$:

$$\frac{\partial \ln \gamma_i}{\partial w_i} = f'_{ij}(\{w\}) = \frac{\partial f_i(\{w\})}{\partial w_j}. \tag{25}$$

Due to the partition of interactions outlined above, the functions f_i incorporate only repulsive interactions, leading to values of $\ln \gamma_i \geqslant 0$ $(\gamma_i \geqslant 1)$ and $\partial \ln \gamma_i/\partial w_j \geqslant 0$. Functions of this type are reviewed and discussed in some detail in Ref. [24]. For purposes of calculating repulsive interactions between globular macrosolutes, each solute species may be represented as an equivalent convex hard particle (sphere, rod, etc.) of size and shape resembling that of the actual molecule at low resolution. In the present work, all species are represented as equivalent hard spheres, so the size of each species is completely specified by the spherical radius r_i. Activity coefficients were calculated using the scaled particle theory of hard sphere fluid mixtures [25].

The calculation of solution composition and signal average buoyant molar mass requires values of the following quantities as input information: the total w/v concentration of solute (w_{tot}), the thermodynamic equilibrium constants (K_i°), the size of the equivalent hard particle representing each species (in the case of an equivalent sphere model, the hard sphere radius r_i), and the buoyant molar mass of each species (M_i^*). Since the apparent equilibrium constants K_i depend in principle upon the solution composition, and since the solution composition depends in principle upon the values of the K_i, the values of both are calculated simultaneously via the following iterative procedure. The values of γ_i, K_i and w_i utilized in the jth iterative step are denoted by $\gamma_i^{(j)}$, $K_i^{(j)}$ and $w_i^{(j)}$, respectively.

1. The values of w_{tot} for which solution compositions are to be calculated are ordered from lowest to highest.
2. For the first iteration $(j=0)$ only: if the particular value of w_{tot} for which the current calculation is being carried out is the first (lowest) value on the list, then $K_i^{(0)}$ is set equal to K_i° for all i. If a previous calculation has been carried out for a lower value of w_{tot}, then the $K_i^{(0)}$ are set equal to the final values of the respective, K_i obtained in the previous calculation.
3. Set $j=j+1$.
4. Set $K_i = K_i^{(j-1)}$, and solve the conservation of mass Eq. (23), either analytically or numerically, to obtain the value of $w_1^{(j)}$.
5. Set $w_1 = w_1^{(j)}$ and evaluate Eq. (22) to obtain the values of all $w_i^{(j)}$.
6. Set $w_i = w_i^{(j)}$ and evaluate Eq. (24) to obtain the values of $K_i^{(j)}$.
7. Set $\gamma_i = \gamma_i^{(j)}$ and evaluate Eq. (22) to obtain the values of $K_i^{(j)}$.
8. Steps 3–7 are repeated iteratively, until the absolute value of $w_i^{(j)} - w_i^{(j-1)}$ is less than some criterion of convergence, selected here to be $0.001 w_{\text{tot}}$, for all species. The final values of K_i, γ_i and w_i so obtained simultaneously satisfy Eqs. (22)–(24).
9. The values of $\partial \ln \gamma_i/\partial w_j$ are calculated using the final values of w_i together with Eq. (25).
10. The elements of array $\underline{\mathbf{A}}$ are calculated using Eq. (6).
11. The values of $M_{i,\text{app}}^*$ are calculated using Eq. (9).
12. The value of M_k^* is calculated using Eq. (13).

4. Experimental materials and methods

Five times crystallized bovine pancreatic ribonuclease A was obtained from Sigma-Aldrich (cat. R-4875) and used without further purification. The protein was equilibrated by extensive dialysis in phosphate-buffered saline (0.05 M sodium phosphate, 0.15 M NaCl, pH 7.4).

At low (<2 g/l) protein concentrations the sedimentation equilibrium experiments were carried in a Optima XL-A analytical ultracentrifuge (Beckman-Coulter Inc., Fullerton, CA) equipped with a UV–VIS scanner, using double-sector 12-mm Epon centerpieces. Ribonuclease samples (70 μl) in phosphate–saline buffer were centrifuged until sedimentation equilibrium at three different speeds (15 000, 18 000 and 23 000 rpm) and 20 °C. The absorbance sedimentation gradients were measured at 275–290 nm. Baseline corrections were determined afterwards by high-speed (50 000 rpm) centrifugation. The apparent weight-average buoyant molar masses were calculated with the programs XLAEQ or EQASSOC (Beckman-Coulter Inc.; see also Ref. [26]), and converted to molar mass using 0.703 cm^3/g as the partial specific volume of ribonuclease [27].

At high (>2 g/l) protein concentrations 70 μl samples were centrifuged at 20 °C to sedimentation equilibrium (4–7 days) at a rotor velocity of 20 000 rpm in a Optima XL ultracentrifuge (Beckman-Coulter) using small polycarbonate tubes and a SW-41 swinging bucket rotor as described earlier [28]. In order to get the corresponding protein gradients, immediately after the conclusion of the centrifugation the contents of each tube were fractionated with a BRANDEL FR-115 centrifuge tube microfractionator (BRANDEL Corp., Gaithersburg, MD) as described earlier [28], and the relative protein concentration in each fraction was determined from the absorbance at 280 nm following dilution of the fractions in buffer to a final absorbance between 0.2 and 1.0 OD unit. High-speed depletion experiments established that no baseline corrections are necessary for this assay. Experiments for each set of experimental conditions were performed in quadruplicate. The corresponding apparent weight-average molar masses were determined by fitting the integrated form of Eq. (11) to the experimental data [20]:

$$S(r) = S(r_o)\exp\left[\frac{\langle M^*_{app}\rangle \omega^2}{2RT}(r^2 - r_o^2)\right] \quad (26)$$

where $S(r)$ is the signal (in this case, absorbance) proportional to the w/v concentration of ribonuclease, r_o is an arbitrarily selected reference position, and $\langle M^*_{app}\rangle$ is the cell-average apparent weight-average buoyant molar mass of ribonuclease.

5. Results

Typical equilibrium gradients of ribonuclease over a broad range of protein concentrations are plotted in Fig. 1, as the linearized transforms of the experimental gradients. The respective calculated best fits of Eq. (11) to calculate the signal-average buoyant molar masses (M^*_{RNase}) are also plotted in Fig. 1. The combined results are plotted in Fig. 2 as the dependence of $M^*_{RNase,app}$ upon ribonuclease concentration. A non-monotonic variation of the slope of the plot is evident, immediately suggesting a combination of self-association and nonideal behavior (cf. Ref. [18]).

We have found that it is possible to fit the data to within experimental uncertainty by a particular case of the general one-component model presented above, in which the protein monomer is assumed to exist in equilibrium with a single oligomeric species designated n-mer, where $n=2$, 3 or 4. The data may also be fitted by a monomer–dimer–tetramer model. The best-fit parameters obtained for each model are presented in Table 1, and the dependence of $M^*_{RNase,app}$ on w_{RNase} calculated using each set of best-fit parameters is plotted together with the data in Fig. 2. Although the monomer–dimer model fits the data, we reject it as physically unrealistic because the best-fit value of r_2/r_1 is less than 1. The weight fractions of each solute species, calculated for the monomer–trimer, monomer–dimer–tetramer and monomer–tetramer models using the respective best-fit parameter values given in Table 1, are plotted as functions of total RNase concentration in Fig. 3.

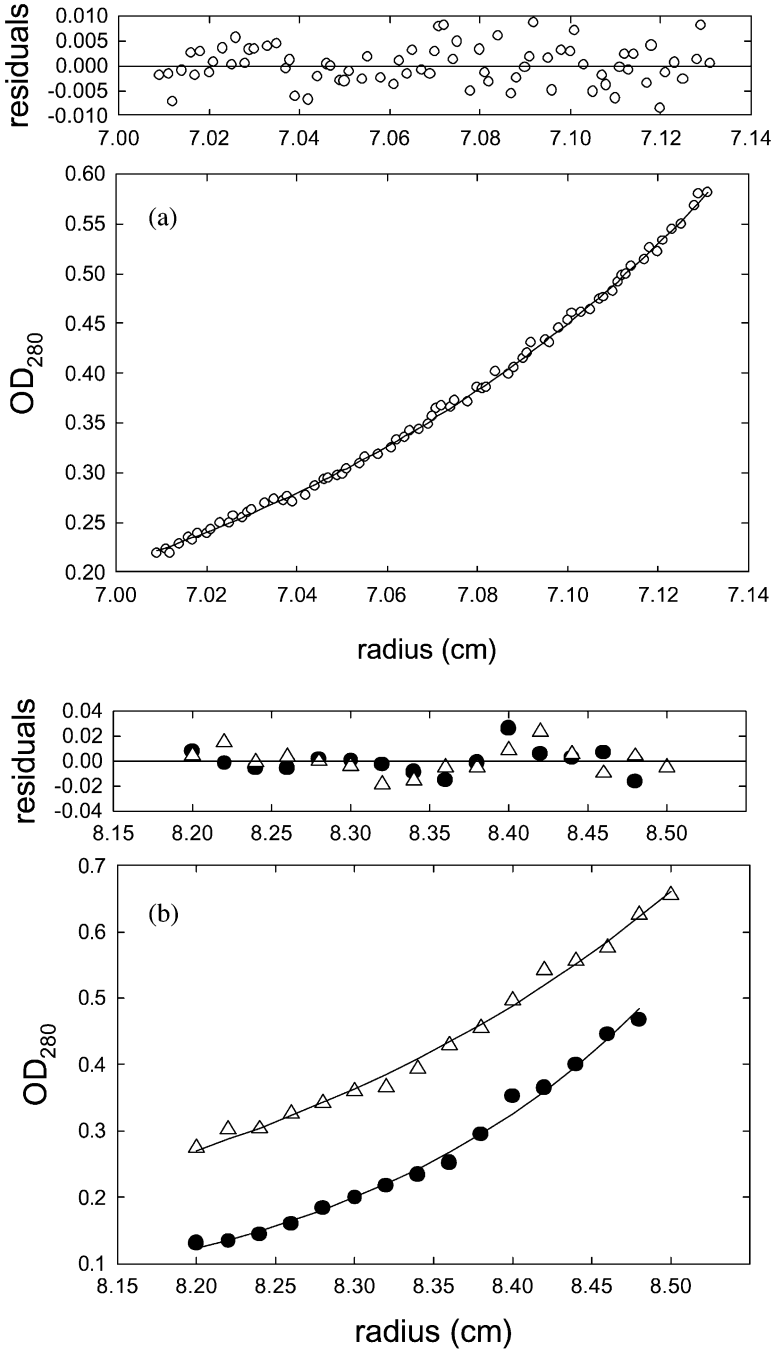

Fig. 1. Representative concentration gradients of ribonuclease at sedimentation equilibrium, measured as described in the text, plotted together with the corresponding best fit of Eq. (11). Open circles: loading concentration 1 g/l, best-fit $M^*_{\mathrm{RNase,app}} = 3800$. Closed circles: loading concentration 25 g/l, best-fit $M^*_{\mathrm{RNase,app}} = 3200$. Triangles: loading concentration 200 g/l, best-fit $M^*_{\mathrm{RNase,app}} = 2300$.

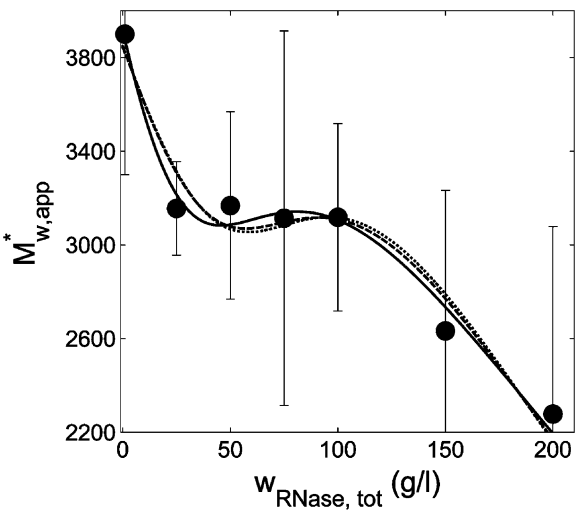

Fig. 2. Dependence of M^*_{RNase} upon protein concentration. Symbols represent the mean and error bars represent ± 2 S.E.M. of 4–6 replicate determinations. Smooth curves are best-fits of monomer–trimer (solid), monomer–dimer–tetramer (long dash) and monomer–tetramer (short dash) models.

6. Discussion

In the present study we have extended theoretical results previously obtained [13,17] and applied experimental techniques previously developed [28] to characterize the state of association of ribonuclease A at concentrations of up to 200 g/l.

Sedimentation equilibrium experiments have been carried out on a number of other concentrated protein solutions. Both normal and sickle hemoglobin have been studied at concentrations up to 370 g/l under a wide variety of conditions [17,29–33]. All of the results are consistent with a simple picture of hemoglobin as an effective hard sphere of molecular size that does not self-associate significantly at any concentration below its solubility limit [32,34].[2] Myoglobin does not appear to self-associate significantly at concentrations under 250 g/l but there is qualitative evidence for very weak self-association at higher concentrations [33]. Analysis of sedimentation equilibrium of defatted monomeric BSA indicates that it does not detectably self-associate in solutions of moderate ionic strength at concentrations up to 200 g/l (unpublished data of D.B. Millar cited in Ref. [15], see also Refs. [17,18]). In contrast, aldolase and ovalbumin, like RNase, were found to exhibit weak but significant self-association at concentrations exceeding 50 g/l in solutions of moderate ionic strength [18].

Muramatsu and Minton [18] employed a semiempirical method suggested by Chatelier and Minton [12] to analyze the concentration dependence of the apparent weight-average molar mass of BSA, aldolase and ovalbumin at concentrations up to 200 g/l. We have reanalyzed these data using the 'exact' general method developed here. The results obtained are presented in Table 2, along with equilibrium constants obtained from the earlier approximate analysis. The best-fit association schemes and estimates of association constants are in excellent agreement with those obtained earlier, and the calculated best-fit dependence of $M^*_{w,\mathrm{app}}$ upon w_{tot} for all three proteins is essentially identical to that plotted in Muramatsu and Minton [18].

[2] Under the conditions of the cited experiments, only the solubility limit of deoxygenated sickle hemoglobin was sufficiently low to be attained experimentally.

Table 1
Best-fit parameters of models for self-association of RNase in nonideal solution

Association scheme	$\log K_n^o$ $(\mathrm{l/g})^{n-1}$	r_1 (Å)	r_n/r_1	WSSR[a]
Monomer–dimer	−2.2	25.6	0.83[b]	0.25
Monomer–trimer	−4.4	19.3	1.31	0.67
Monomer–dimer–tetramer	−2.6 ($n=2$), −6.6 ($n=4$)	18.5	1.26 ($n=2$, constrained) 1.58 ($n=4$, constrained)	2.84
Monomer–tetramer	−6.7	15.3	1.90	3.17

[a] Weighted sum of squared residuals.
[b] Value unacceptably small on physical grounds.

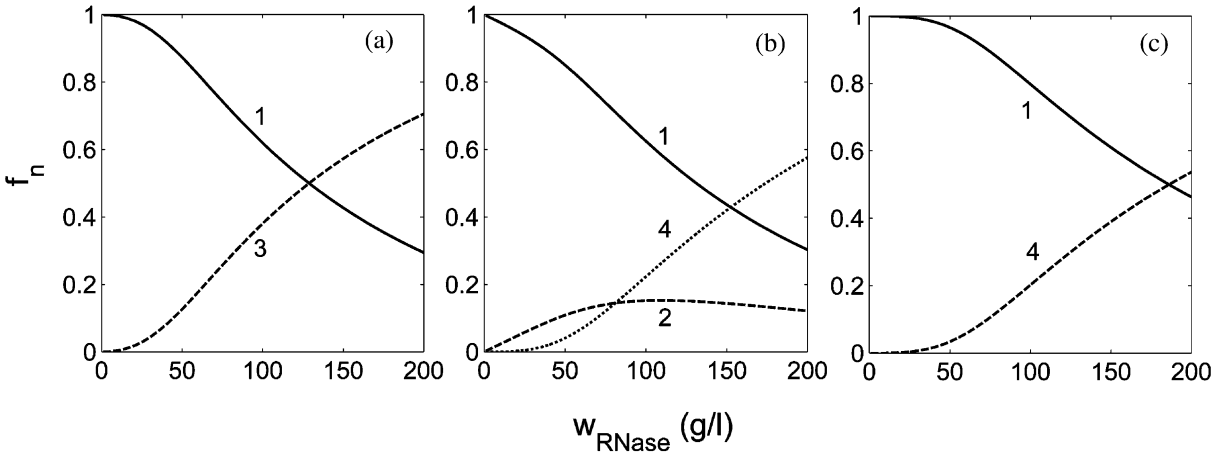

Fig. 3. Weight fractions of ribonuclease species, calculated as a function of total protein concentration for the monomer–trimer (panel A), monomer–dimer–tetramer (panel B) and monomer–tetramer models (panel C), using the best fit parameter values given in Table 1.

This close agreement attests to the validity of the semiempirical approximations suggested earlier by Chatelier and Minton [12].

The data presented here may be accommodated to within experimental precision by a simple model for monomer in equilibrium with a trimer, a tetramer or a dimer and tetramer mixture, coupled with repulsion between species represented by effective hard spheres. It is emphasized that the self-association detected in the present experiments is extremely weak (e.g. K_2 is of the order of 20–50/M), and the association products are probably entirely unrelated to the RNase dimers that have been reported to be formed by domain swapping under considerably different experimental conditions [35,36].

The present data do not allow us to select a unique model for self-association, although the monomer–dimer–tetramer model seems most appealing on the grounds that the relative sizes of effective hard spheres representing the three species correspond exactly to volume (mass) ratios of 1:2:4. The actual situation may be more complex, involving significant nonideal interaction over and above steric repulsion. Further progress in elucidating these factors will require a significantly more precise experimental determination of the dependence of $M^*_{w,\mathrm{app}}$ upon w_{tot}. This in turn

Table 2
Best-fit parameters derived from current analysis and original approximate analysis of the data of Muramatsu and Minton (1989)

Protein	Association scheme	Original analysis [18]	Current analysis		
		$\log K_n^{\circ}$ $(\mathrm{l/g})^{n-1}$	$\log K_n^{\circ}$ $(\mathrm{l/g})^{n-1}$	r_1 (Å)	r_n/r_1
BSA	No self-association	n.a.	n.a.	30.4	n.a.
Aldolase	Monomer–dimer	−2.1	−2.2	32.2	1.45
Aldolase	Monomer–trimer[a]	−3.9	−4.1	27.4	2.65
Ovalbumin	Monomer–trimer	−3.05	−3.05	29.7	1.29

[a] Although the monomer–trimer model is acceptable on grounds of goodness of fit, the best-fit radius of the effective hard sphere representing trimer corresponds to a volume approximately 20-fold greater than that of the particle representing monomer. Although this apparent increase in exclusion volume may reflect, in part, a significantly nonspherical conformation of trimer [24], the monomer–dimer model appears to provide a more realistic description of the association of aldolase. This difference between the two models was not evident in the earlier analysis.

requires both more precise evaluation of $M^*_{w,app}$ at each total concentration of w_{tot}, as well as more gradients acquired over smaller intervals of total concentration. In spite of the limited precision of the present experimental results, these data, together with our analysis, clearly and unambiguously establish the presence and importance of both weak self-association and thermodynamic nonideality in defining the composition and the sedimentation equilibrium of solutions of ribonuclease A in concentrated solution.

Acknowledgments

This work was supported in part by research grants from the Spanish Ministry of Science and Technology (BIO99-0859-C03-03, BMC2002-04617-C02-01 and BQU2000-1500) and the *Programa de Grupos Estratégicos* of the Government of Madrid. Silvia Zorrilla was a predoctoral fellow of the Government of Madrid. We thank Dr Carlos Alfonso (CIB-CSIC) for performing the sedimentation equilibrium experiments with the analytical ultracentrifuge.

References

[1] A. Minton, Quantitative characterization of reversible molecular associations via analytical ultracentrifugation, Anal. Biochem. 190 (1990) 1–6.
[2] G. Rivas, W. Stafford, A. Minton, Characterization of heterologous protein–protein interactions using analytical ultracentrifugation, Methods 19 (1999) 194–212.
[3] A.B. Fulton, How crowded is the cytoplasm?, Cell 30 (1982) 345–347.
[4] S.B. Zimmerman, A.P. Minton, Macromolecular crowding: biochemical, biophysical, and physiological consequences, Annu. Rev. Biophys. Biomol. Struct. 22 (1993) 27–65.
[5] A.P. Minton, Excluded volume as a determinant of macromolecular structure and reactivity, Biopolymers 20 (1981) 2093–2120.
[6] R.J. Ellis, Macromolecular crowding: obvious but underappreciated, Trends Biochem. Sci. 26 (2001) 597–604.
[7] A.P. Minton, The influence of macromolecular crowding and macromolecular confinement on biochemical reactions in physiological media, J. Biol. Chem. 276 (2001) 10577–10580.
[8] H. Knull, A.P. Minton, Structure within eukaryotic cytoplasm and its relationship to glycolytic metabolism, Cell Biochem. Funct. 14 (1996) 237–248.
[9] P. Wills, M. Jacobsen, D. Winzor, Analysis of sedimentation equilibrium distributions reflecting nonideal macromolecular associations, Biophys. J. 79 (2000) 2178–2187.
[10] J. Behlke, O. Ristau, Analysis of protein self-association under conditions of the thermodynamic non-ideality, Biophys. Chem. 87 (2000) 1–13.
[11] P. Wills, D. Winzor, Studies of solute self-association by sedimentation equilibrium: allowance for effects of thermodynamic non-ideality beyond the consequences of nearest-neighbor interactions, Biophys. Chem. 91 (2001) 253–262.
[12] R.C. Chatelier, A.P. Minton, Sedimentation equilibrium in macromolecular solutions of arbitrary concentration. I. Self-associating proteins, Biopolymers 26 (1987) 507–524.
[13] R.C. Chatelier, A.P. Minton, Sedimentation equilibrium in macromolecular solutions of arbitrary concentration. II. Two protein components, Biopolymers 26 (1987) 1097–1113.
[14] G. Rivas, J.A. Fernández, A.P. Minton, Direct observation of the self-association of dilute proteins in the presence of inert macromolecules at high concentration via tracer sedimentation equilibrium: theory, experiment, and biological significance, Biochemistry 38 (1999) 9379–9388.
[15] A.P. Minton, The effect of volume occupancy upon the thermodynamic activity of proteins: some biochemical consequences, Mol. Cell. Biochem. 55 (1983) 119–140.
[16] D.R. Hall, A.P. Minton, Macromolecular crowding: qualitative and semi-quantitative successes, quantitative challenges', Biochim. Biophys. Acta 1649 (2003) 127–139.
[17] G. Rivas, J.A. Fernández, A.P. Minton, Direct observation of the enhancement of non-cooperative protein assembly by macromolecular crowding: indefinite self-association of the bacterial cell division protein FtsZ, Proc. Natl. Acad. Sci. USA 98 (2001) 3150–3155.
[18] N. Muramatsu, A.P. Minton, Hidden self-association of proteins, J. Mol. Recog. 1 (1989) 166–171.
[19] H. Eisenberg, Analytical ultracentrifugation in a Gibbsian perspective, Biophys. Chem. 88 (2000) 1–9.
[20] A.P. Minton, Alternative strategies for the characterization of associations in multicomponent solutions via measurement of sedimentation equilibrium, Prog. Colloid Polym. Sci. 107 (1997) 11–19.
[21] C. Tanford, Physical Chemistry of Macromolecules, Academic Press, New York, 1961.
[22] W.G. McMillan Jr., J.E. Mayer, The statistical thermodynamics of multicomponent systems, J. Chem. Phys. 13 (1945) 276–305.
[23] T.L. Hill, Y.D. Chen, Theory of aggregation in solution. I. General equations and application to the stacking of bases, nucleotides, etc, Biopolymers 12 (1971) 1285–1312.
[24] A.P. Minton, Molecular crowding: analysis of effects of high concentrations of inert cosolutes on biochemical

equilibria and rates in terms of volume exclusion, Methods Enzymol. 206 (1998) 127–149.

[25] J.L. Lebowitz, E. Helfand, E. Praestgaard, Scaled particle theory of fluid mixtures, J. Chem. Phys. 43 (1965) 774–779.

[26] A.P. Minton, in: T.M. Schuster, B. Laue (Eds.), Modern Analytical Ultracentrifugation, Birkhäuser, Boston, 1994, pp. 81–93.

[27] F.M. Richards, H.W. Wyckoff, in: P.D. Boyer (Ed.), The Enzymes, Academic Press, New York, 1971, pp. 647–806.

[28] S. Darawshe, G. Rivas, A.P. Minton, Rapid and accurate microfractionation of the contents of small centrifuge tubes: application in the measurement of molecular weights of proteins via sedimentation equilibrium, Anal. Biochem. 209 (1993) 130–135.

[29] J. Sophianopoulos, A. Sophianopoulos, J. Knowles, R. Hill, Solubility of hemoglobin S by sedimentation equilibrium, and antisickling compounds, Arch. Biochem. Biophys. 173 (1976) 517–527.

[30] R. Williams Jr., Concerted formation of the gel of HbS, Proc. Natl. Acad. Sci. USA 70 (1973) 1506–1508.

[31] R. Briehl, S. Ewert, Effects of pH, 2,3-DPG and salts on gelation of sickle cell deoxyhemoglobin, J. Mol. Biol. 80 (1973) 445–458.

[32] P.D. Ross, R.W. Briehl, A.P. Minton, Temperature dependence of nonideality in concentrated solutions of hemoglobin, Biopolymers 17 (1978) 2285–2288.

[33] A.P. Minton, M.S. Lewis, Self-association in highly concentrated solutions of myoglobin: a novel analysis of sedimentation equilibrium of highly nonideal solutions, Biophys. Chem. 14 (1981) 317–324.

[34] P. Ross, A. Minton, Analysis of nonideal behavior in concentrated hemoglobin solutions, J. Mol. Biol. 112 (1977) 437–452.

[35] Y. Liu, P. Hart, M. Schlunegger, D. Eisenberg, The crystal structure of a 3D domain-swapped dimer of RNase A at a 2.1 A resolution, Proc. Natl. Acad. Sci. USA 95 (1998) 3437–3442.

[36] C. Park, R. Raines, Dimer formation by a 'monomeric' protein, Protein Sci. 9 (2000) 2026–2033.